Influence of hardening on the cyclic behavior of laminate microstructures in finite crystal plasticity

D. M. Kochmann, K. Hackl

We investigate the cyclic behavior of laminate microstructures in finite-strain crystal plasticity and the resulting stress-strain response, based on a variational, incremental description of the microstructure evolution. The non-convex free energy density in multiplicative single- and multi-slip plasticity gives rise to the formation of fine-scale deformation structures, experimentally observed as complex material microstructures. Here, we treat first-order laminate microstructures and model their origin and their subsequent evolution. Interestingly, the cyclic behavior of such microstructures has been reported to exhibit a gradual degeneration of the laminate as well as of the stress-strain hysteresis loop, leading to an elastic shakedown. However, previous results have predicted the occurrence of this final, steady state within a few load cycles, which has appeared physically doubtful. Therefore, we analyze here the influence of work hardening in single-slip and of latent hardening in double-slip plasticity on the laminate microstructures and the corresponding stress-strain responses during cyclic loading. Results indicate that the amount of hardening considerably affects the rate at which the stress-strain hysteresis and the laminate degenerate.

1 Introduction

The mechanical properties of materials in science and engineering are essentially linked to their microstructures. The occurrence of ordered, hierarchical, or randomly distributed arrangements of dislocations and other lattice defects to form a complex network on the microscale results in a distinct overall, effective response of the material body deforming elastoplastically under the action of external forces. Experiments indicate that very often the assembly of the microstructural components are not completely random but rather form specific patterns and regular arrays. Simple examples include laminate-type structures of alternating deformation domains (Dmitrieva et al., 2009), as can also be found e.g. in shear bands or deformation twins (Christian and Mahajan, 1995), or labyrinth-type structures (Jin and Winter, 1984). In all of these examples dislocations align along preferred crystallographic orientations, thus forming complex systems of dislocation walls (Ortiz and Repetto, 1999). In opposition to the enormous variety of such observed microstructures stands their tantamount influence on the macroscopic material behavior. Therefore, the development of patterns and structures on the microscale is of crucial importance, which requires careful investigation not only in order to analyze and comprehend the experimentally observed geometrical specifics of prevalent microstructures but also to predict the arising macroscopic response and thus to design material properties by demand.

The accommodation of plastic deformation by complex interactions of the dislocation network is governed by the concepts of free energy and dissipation. A deformed solid stores energy both in the elastically strained lattice as well as in the long-range distortion fields of dislocations, whose motion transforms energy into heat (i.e., dissipates stored energy). Based on the thermodynamic concept of energy minimization, the origin of microstructural patterns has been understood as the realization of energy-minimizing sequences for non-convex energy landscapes (Ball, 1977; Ball and James, 1987; Truskinovsky and Zanzotto, 1995; Govindjee et al., 2003). Ericksen (1975) was among the first to conclude microstructural patterns as a direct result of energy minimum principles applied to multi-welled strain-energy densities, whose idea was transformed later into a more complex theory predominantly for the treatment of phase transformations (Govindjee et al., 2003) and problems in elasto-plasticity (Ortiz and Repetto, 1999; Carstensen et al., 2002). As a consequence of the non-(quasi)convex energy, the material body, aiming to reduce its energy, does not respond by means of a homogeneous deformation state but breaks up into multiple deformation domains at local energy minima in order to further reduce the overall stored energy in such a way which is compatible with the overall imposed deformation field. Solutions to describe these domain mixtures have been developed by employing the theory of relaxation to find the quasiconvex hull of the free energy (Morrey,

1952). By considering associated potentials in a time-incremental setting, several authors have investigated the initiation of microstructures via relaxation (Ortiz and Repetto, 1999; Lambrecht et al., 2003; Dolzmann, 2003; Mielke, 2004; Bartels et al., 2004; Conti and Theil, 2005; Carstensen et al., 2008), using a condensed energy functional. This method has been applied successfully to the evolution of inelastic materials, see (Mielke and Ortiz, 2007; Conti and Ortiz, 2008). An incremental energy minimization strategy has been outlined by Miehe et al. (2004) and applied to the evolution of first-order laminates in single-slip plasticity.

Modeling the macroscopic material behavior during microstructure formation not only involves knowledge about the origin of such structures but also requires a physically well-reasoned concept to treat the subsequent evolution of an existing microstructure. This has often been addressed in the literature by employing condensed energy functionals to approximate the evolution of such structures in time, which, however, faces several difficulties. On the one hand, the use of a condensed energy functional in a single time step can only be an approximate solution since it does not account for all microstructural changes during each small time increment with already existing microstructure at the beginning. On the other hand, the application of a condensed energy functional requires an explicit expression of the dissipation distance, which often does not appear feasible already when more than one slip system is active (Hackl et al., 2003). Also, non-monotonous load conditions (e.g. cyclic loading) requires an incremental modeling strategy, which can be achieved only in an approximated manner when using condensed functionals. To overcome these problems, we have developed an incremental formulation based on the iterative solution of the evolution equations for the internal variables which capture the microstructural characteristics (Hackl and Kochmann, 2008; Kochmann and Hackl, 2009a). This incremental method has been applied successfully to monotonous (Hackl and Kochmann, 2008) and cyclic loading (Kochmann and Hackl, 2009a) of single-slip single-crystals. In particular, results from single-slip cyclic tests have demonstrated the interesting feature of a rapidly decaying stress-strain hysteresis within a few cycles to eventually lead to an almost steady microstructure with hardly changing characteristics (Hackl and Kochmann, 2009), i.e., it comes to an elastic shakedown. Although observed experimentally e.g. for copper single crystals, the predicted cyclic behavior from the present model has appeared unrealistic, since the steady state is reached after a few load cycles only and the changes between subsequent cycles appear too abrupt. It has been theorized (but not investigated yet) that the influence of work hardening as well as the activation of multiple slip systems and the correlated latent hardening play an important role with considerable impact on the cyclic behavior.

Here, we briefly review the mathematical and numerical set-up of the incremental, variational formulation of laminate microstructures in crystal plasticity, which will be employed to scrutinize the influence of hardening on the cyclic performance of laminate patterns. We therefore discuss the incorporation of hardening into the constitutive framework and the implementation of several active slip systems. Then, we present numerical examples of single- and double-slip plasticity of cyclically-loaded single crystals to illustrate the importance of work hardening.

2 Variational constitutive formulation

Following (Hackl and Kochmann, 2008), we describe the isothermal state of an inelastic solid by its deformation gradient $\boldsymbol{F} = \nabla \phi$, resulting from the displacement field $\phi(\boldsymbol{X})$, and a collection of internal variables $\boldsymbol{z}(\boldsymbol{X})$, which capture all microstructural specifics. The specific Helmholtz free energy density $\Psi(\boldsymbol{F}, \boldsymbol{z})$ is introduced, resulting in the thermodynamically conjugate stresses

$$\boldsymbol{P} = \frac{\partial \Psi}{\partial \boldsymbol{F}}, \qquad \boldsymbol{Q} = -\frac{\partial \Psi}{\partial \boldsymbol{z}}, \tag{1}$$

with $\boldsymbol{P}$ being the first Piola-Kirchhoff stress tensor. The evolution of the internal variables is governed either by an inelastic potential $J(\boldsymbol{z}, \boldsymbol{Q})$ (plasticity models commonly use an indicator function linked to the yield surface) or its Legendre-transform (Carstensen et al., 2002), the dissipation functional

$$\Delta(\boldsymbol{z}, \dot{\boldsymbol{z}}) = \sup \left\{ \dot{\boldsymbol{z}} : \boldsymbol{Q} - J(\boldsymbol{z}, \boldsymbol{Q}) \,\middle|\, \boldsymbol{Q} \right\}, \tag{2}$$

where the dot denotes differentiation with respect to time. The evolution equations for the internal variables are then given in either of the two equivalent forms

$$\dot{\boldsymbol{z}} \in \frac{\partial J}{\partial \boldsymbol{Q}}, \qquad \boldsymbol{Q} \in \frac{\partial \Delta}{\partial \dot{\boldsymbol{z}}}, \tag{3}$$

from which the latter differential inclusion constitutes a rephrasal of the well-known Biot equation of standard generalized materials (Biot, 1965; Germain, 1973; Ziegler and Wehrli, 1987; Nguyen, 2000). The complete evolution

problem can now be described in terms of two minimum principles where we follow ideas presented by Ortiz and Repetto (1999), Carstensen et al. (2002) and Mielke (2002). We denote the total free energy of the body by

$$\mathcal{I}(t, \boldsymbol{\phi}, \boldsymbol{z}) = \int_{\Omega} \Psi(\nabla\boldsymbol{\phi}, \boldsymbol{z}) \, \mathrm{d}v - \ell(t, \boldsymbol{\phi}) \tag{4}$$

where $\ell(t, \boldsymbol{\phi})$ represents the potential of external forces, and Ω is the body's volume. The actual displacement field then follows from the principle of minimum potential energy

$$\boldsymbol{\phi} = \operatorname{argmin} \left\{ \, \mathcal{I}(t, \boldsymbol{\phi}, \boldsymbol{z}) \mid \boldsymbol{\phi} = \boldsymbol{\phi}_0 \text{ on } \Gamma_{\boldsymbol{u}} \, \right\}, \tag{5}$$

with boundary conditions $\boldsymbol{\phi}_0$ prescribed on the subset $\Gamma_{\boldsymbol{u}}$ of the body's boundary $\partial\Omega$.

It is convenient to introduce a Lagrange functional consisting of the sum of the energy rate and the dissipation potential (sometimes referred to as the total power)

$$\mathcal{L}(\boldsymbol{\phi}, \boldsymbol{z}, \dot{\boldsymbol{z}}) = \frac{\mathrm{d}}{\mathrm{d}t} \Psi(\nabla\boldsymbol{\phi}, \boldsymbol{z}) + \Delta(\boldsymbol{z}, \dot{\boldsymbol{z}}). \tag{6}$$

The evolution of the internal variables is then governed by the minimum principle (Ortiz and Repetto, 1999; Carstensen et al., 2002)

$$\dot{\boldsymbol{z}} = \operatorname{argmin} \left\{ \, \mathcal{L}(\boldsymbol{\phi}, \boldsymbol{z}, \dot{\boldsymbol{z}}) \mid \dot{\boldsymbol{z}} \, \right\}, \tag{7}$$

It has been shown (Hackl and Fischer, 2007) that for dissipation potentials which are homogeneous of degree n (as e.g. in rate-independent plasticity) the above principle (7) is equivalent to the principle of maximum dissipation (i.e., of maximum entropy production). The above two minimum principles can be applied in order to compute the time-continuous evolution of both the elastic and plastic variables.

Unfortunately, typical problems of elastoplasticity as well as of phase-transforming materials encounter energy densities which are not (quasi-)convex so that no minimizer in terms of a homogeneous deformation state exists. Instead, those materials can accommodate a lowest-energy state by breaking up into multiple domains at local energy minima, forming characteristic structures and patterns to reduce the crystal's energy. The description and simulation of these microstructures requires knowledge about the quasiconvex envelope of the free energy density, which is defined by

$$Q\Psi(\boldsymbol{F}) = \inf \left\{ \frac{1}{|\omega|} \int_{\omega} \Psi(\boldsymbol{F} + \boldsymbol{\nabla}\boldsymbol{\varphi}) \, \mathrm{d}V \mid \boldsymbol{\varphi} \, : \, \boldsymbol{\varphi} = \boldsymbol{0} \text{ on } \partial\omega \right\} \tag{8}$$

for arbitrary bounded sets ω. Here, $\boldsymbol{\varphi}$ denotes a small-scale fluctuation field which describes the energy-minimizing microstructure. Replacing the non-convex energy density in the above variational framework by its quasiconvex hull renders the minimization problem well-posed while pre-accounting for all admissible microstructures.

As the computation of the quasiconvex hull in general does not appear feasible, it has been replaced by appropriate upper and lower bounds in terms of the rank-one-convex and the polyconvex hull, respectively. Besides, the rank-one-convex hull $R\Psi(\boldsymbol{F})$ allows for a neat geometrical interpretation as a laminate structure. It is defined recursively, beginning with the first-order laminate energy

$$R_1\Psi(\boldsymbol{F}) = \inf \left\{ (1-\lambda)\Psi(\boldsymbol{F}_1) + \lambda\Psi(\boldsymbol{F}_2) \mid \lambda, \boldsymbol{F}_i \, ; \, (1-\lambda)\boldsymbol{F}_1 + \lambda\boldsymbol{F}_2 = \boldsymbol{F}, \, \operatorname{rank}(\boldsymbol{F}_1 - \boldsymbol{F}_2) \leq 1 \right\}, \tag{9}$$

which corresponds to a first-order laminate consisting of two domains with volume fractions λ and $1-\lambda$ and constant deformation gradients $\boldsymbol{F}_1$ and $\boldsymbol{F}_2$ within the domains 1 and 2, respectively. Repeating the above construction within each laminate domain, one arrives at higher-order laminates (see Figure 1a-d) with the corresponding hulls $R_k\Psi = R_1^k\Psi$. This refinement can be performed numerically (Dolzmann, 1999). The rank-one-convex hull then follows from

$$R\Psi = \lim_{k \to \infty} R_k\Psi. \tag{10}$$

As experiments very often indicate the formation of first-order laminate structures only, see e.g. (Dmitrieva et al., 2009), we will restrict in the sequel to this particular geometrical type of microstructures and hence employ $R_1\Psi(\boldsymbol{F})$ to replace the non-(quasi)convex energy density. In particular, we will make use of laminated Young measures to describe the microstructural characteristics; the interested reader is referred to (Hackl and Kochmann, 2008; Kochmann and Hackl, 2009a).

Finally, it has proved convenient to reformulate the minimum principle (7) in an integral setting by introducing the dissipation distance (Mielke, 2002) for a finite time increment $[t_n, t_{n+1}]$,

$$D(\boldsymbol{z}_0, \boldsymbol{z}_1) = \inf \left\{ \int_0^1 \Delta(\boldsymbol{z}(s), \dot{\boldsymbol{z}}(s)) \, \mathrm{d}s \mid \boldsymbol{z}(0) = \boldsymbol{z}_0, \boldsymbol{z}(1) = \boldsymbol{z}_1 \right\}. \tag{11}$$

In rate-independent plasticity an approximate formulation for the above minimization problem is then given in terms of the condensed energy

$$\Psi_{\boldsymbol{z}_n}^{\mathrm{cond}}(\boldsymbol{F}) = \inf \left\{ \Psi(\boldsymbol{F}, \boldsymbol{z}) + D(\boldsymbol{z}_n, \boldsymbol{z}) \,\middle|\, \boldsymbol{z} \right\}, \tag{12}$$

which has been used in the literature to calculate the onset of microstructures and to model the subsequent microstructure evolution (Ortiz and Repetto, 1999; Miehe et al., 2002; Lambrecht et al., 2003; Bartels et al., 2004; Conti and Theil, 2005). However, the use of the condensed energy functional is restricted to simple problems where the dissipation distance is available. Also, it does not account for all actual microstructural changes during a time step with already existing microstructure at the beginning of the time step, as will be discussed in the sequel.

3   Laminate microstructures in crystal plasticity

In finite elastoplasticity the deformation gradient decomposes into its elastic and plastic contribution as $\boldsymbol{F} = \boldsymbol{F}_{\mathrm{e}} \boldsymbol{F}_{\mathrm{p}}$. The plastic contribution is accommodated by dislocation slip along certain active slip systems, which are characterized by their slip directions $\boldsymbol{s}_i$ and the slip plane normals $\boldsymbol{m}_i$ ($|\boldsymbol{s}_i| = |\boldsymbol{m}_i| = 1$, $\boldsymbol{s}_i \cdot \boldsymbol{m}_i = 0$). For a total of n active slip systems the plastic flow rule follows as

$$\dot{\boldsymbol{F}}_{\mathrm{p}} \boldsymbol{F}_{\mathrm{p}}^{-1} = \sum_{i}^{n} \dot{\gamma}_i \, \boldsymbol{s}_i \otimes \boldsymbol{m}_i \tag{13}$$

with plastic slip rates $\dot{\gamma}_i$ and the initial conditions $\gamma_i(0) = 0$. Time-integration then yields the plastic contribution to the deformation gradient tensor, which becomes quite complex and hence cannot be performed analytically in general (Hackl et al., 2003). However, if we assume e.g. that all slip directions lie within the same slip plane, i.e. $\boldsymbol{m}_i = \boldsymbol{m}$, we obtain because of $\boldsymbol{s}_i \cdot \boldsymbol{m} = 0$ the handy form (Carstensen et al., 2002)

$$\boldsymbol{F}_{\mathrm{p}}^{-1} = \mathbf{I} - \sum_{i}^{n} \gamma_i \, \boldsymbol{s}_i \otimes \boldsymbol{m}. \tag{14}$$

For the following model problems in crystal plasticity we will employ a Neo-Hookean energy density and, in order to allow for a closed-form semi-analytical relaxation, assume incompressible material behavior, i.e., $\det \boldsymbol{F}_{\mathrm{e}} = \det \boldsymbol{F} = 1$ (this assumption is justified when the elastic strains are small compared to the volume-preserving plastic strains). To account for work hardening, we introduce internal hardening history variables p_i (Carstensen et al., 2002), one such hardening variable for each active slip system, abbreviated by $\boldsymbol{p} = \{p_1, \ldots, p_n\}$. The hardening variables are responsible for the plastic (intrinsic) contribution to the energy and evolve with changes of the plastic slip via the flow rule $\dot{p}_i = |\dot{\gamma}_i|$ with the initial condition $p_i(0) = 0$ (virgin initial state). With all of these model assumptions and definitions we can formulate the total free energy density of our model:

$$\Psi(\boldsymbol{F}_{\mathrm{e}}, \boldsymbol{p}) = \frac{\mu}{2} \left(\operatorname{tr} \boldsymbol{F}_{\mathrm{e}}^{T} \boldsymbol{F}_{\mathrm{e}} - 3 \right) + \sum_{i}^{n} \sum_{j}^{n} \kappa_{ij} \, |p_i \, p_j|^{\alpha/2}, \qquad \det \boldsymbol{F} = 1. \tag{15}$$

The first term represents the stored elastic energy of the incompressible Neo-Hookean material, the second term characterizes the intrinsically stored energy, where $\kappa_{ij} > 0$ are the components of a hardening modulus tensor of the material and α is commonly 2 (linear hardening) or 4. Self-hardening along any of the slip systems is captured by the diagonal entries κ_{ii}, whereas latent hardening (slip system interactions due to cross-slip etc.) involves the off-diagonal components κ_{ij} ($i \neq j$). Experiments confirm that the off-diagonal entries should dominate.

Is has been shown (Hackl and Kochmann, 2008, 2009; Kochmann and Hackl, 2009b) that the free energy density (15) is non-(quasi)convex in general so that microstructures arise to reduce the energy. As an approximation appropriate for many experimental findings, we assume the formation of a laminate of first order, which is characterized by N domains with volume fractions λ_i, separated by parallel planes with normal vector $\boldsymbol{b}$, as sketched in Figure 1e. To each domain i there correspond values γ_{ij} and p_{ij} of the internal variables for each active slip system j. Moreover, in every domain we have a constant deformation gradient $\boldsymbol{F}_i$ which will for convenience be defined by

$$\boldsymbol{F}_i = \boldsymbol{F}(\mathbf{I} + \boldsymbol{a}_i \otimes \boldsymbol{b}). \tag{16}$$

This formulation ensures that deformation gradients differ only by tensors of rank one, enforcing compatibility at laminate interfaces and hence ensuring the existence of a corresponding deformation field. The vector $\boldsymbol{b}$ is the unit

normal to the laminate interfaces (the orientation vector) and $\boldsymbol{a}_i$ represents some deformation amplitude vector. We impose the volume average of the deformation gradient

$$\sum_{i=1}^{N} \lambda_i \boldsymbol{F}_i = \boldsymbol{F} \qquad \Leftrightarrow \qquad \sum_{i=1}^{N} \lambda_i \boldsymbol{a}_i = \boldsymbol{0}. \tag{17}$$

Furthermore, we must ensure incompressibility of each laminate domain, according to the above assumption, i.e.,

$$\det \boldsymbol{F}_i = 1 \qquad \Leftrightarrow \qquad \boldsymbol{a}_i \cdot \boldsymbol{b} = 0. \tag{18}$$

Let us now introduce the semi-relaxed energy density. We consider the orientation vector $\boldsymbol{b}$ as ingrained into the material, since changes of the orientation would require a rearrangement of the microstructure, thus leading to dissipation. The amplitudes $\boldsymbol{a}_i$, on the other hand, can be changed purely elastically. Taking into account the constraints (17) and (18) by introducing Lagrange multipliers $\boldsymbol{\Lambda}$ and ρ_i, the semi-relaxed elastic energy be defined by

$$\Psi_{\mathrm{el}}^{\mathrm{rel}}(\boldsymbol{F}, \lambda_i, \gamma_{ij}, \boldsymbol{b}) = \inf \left\{ \frac{\mu}{2} \sum_i^{N} \lambda_i \left[\operatorname{tr} \boldsymbol{C}_{\mathrm{e},i} - 3 - 2\boldsymbol{\Lambda} \cdot \boldsymbol{a}_i - 2\rho_i \boldsymbol{a}_i \cdot \boldsymbol{b} \right] \middle| \boldsymbol{a}_i \right\}, \tag{19}$$

where $\boldsymbol{C} = \boldsymbol{F}^\mathsf{T} \boldsymbol{F}$ denotes the right Cauchy-Green tensor and $\boldsymbol{C}_{\mathrm{e},i} = \boldsymbol{F}_{\mathrm{e},i}^\mathsf{T} \boldsymbol{F}_{\mathrm{e},i}$ the elastic Cauchy-Green tensor in the domain i with, following (14) and (16),

$$\boldsymbol{F}_{\mathrm{e},i} = \boldsymbol{F}_i \boldsymbol{F}_{\mathrm{p},i}^{-1} = \boldsymbol{F}(\boldsymbol{I} + \boldsymbol{a}_i \otimes \boldsymbol{b}) \left(\boldsymbol{I} - \sum_j^{n} \gamma_{ij} \boldsymbol{s}_j \otimes \boldsymbol{m} \right), \tag{20}$$

Minimization in (19) with respect to the unknown quantities $\boldsymbol{a}_i$ can be carried out analytically to yield

$$\Psi_{\mathrm{el}}^{\mathrm{rel}}(\boldsymbol{F}, \lambda_i, \gamma_{ij}, \boldsymbol{b}) = \frac{\mu}{2} \left[\operatorname{tr} \boldsymbol{C} - 3 + \frac{1}{\sum_i^N \frac{\lambda_i}{\boldsymbol{b}_i \cdot \boldsymbol{b}}} \left(\sum_j^N \sum_k^N \frac{\lambda_j \lambda_k \boldsymbol{b}_j \cdot \boldsymbol{C} \boldsymbol{b}_k}{\boldsymbol{b}_j \cdot \boldsymbol{b}\, \boldsymbol{b}_k \cdot \boldsymbol{b}} - \frac{1}{\boldsymbol{b} \cdot \boldsymbol{C}^{-1} \boldsymbol{b}} \right) \right.$$
$$\left. + \sum_i^N \lambda_i \left(\frac{\boldsymbol{b}_i \cdot \boldsymbol{b}}{\boldsymbol{b} \cdot \boldsymbol{C}^{-1} \boldsymbol{b}} - \frac{\boldsymbol{b}_i \cdot \boldsymbol{C} \boldsymbol{b}_i}{\boldsymbol{b}_i \cdot \boldsymbol{b}} \right) + \sum_i^N \lambda_i \operatorname{tr} \left(\boldsymbol{F}_{\mathrm{p},i}^{-T} \boldsymbol{C} \boldsymbol{F}_{\mathrm{p},i}^{-1} \right) \right] \tag{21}$$

with

$$\boldsymbol{b}_i = \boldsymbol{b} \cdot \boldsymbol{F}_{\mathrm{p},i}^{-T} \boldsymbol{F}_{\mathrm{p},i}^{-1}. \tag{22}$$

The most general case for which $\boldsymbol{F}_\mathrm{p}$ can be given analytically requires the assumption that all slip systems in one domain lie within the same glide plane ($\boldsymbol{m}_i = \boldsymbol{m}$), so that the above abbreviations reduce to

$$\boldsymbol{b}_i = \boldsymbol{b} - \sum_j^{n} \gamma_{ij}(\boldsymbol{b} \cdot \boldsymbol{m}\, \boldsymbol{s}_{ij} + \boldsymbol{b} \cdot \boldsymbol{s}_{ij}\, \boldsymbol{m}) + \sum_j^{n} \gamma_{ij}^2\, \boldsymbol{b} \cdot \boldsymbol{s}_{ij}\, \boldsymbol{s}_{ij},$$

$$\operatorname{tr} \left(\boldsymbol{F}_{\mathrm{p},i}^{-T} \boldsymbol{C} \boldsymbol{F}_{\mathrm{p},i}^{-1} \right) = \sum_j^{n} \left(\gamma_{ij}^2\, \boldsymbol{s}_j \cdot \boldsymbol{C} \boldsymbol{s}_j - 2\, \gamma_{ij}\, \boldsymbol{s}_j \cdot \boldsymbol{C} \boldsymbol{m} \right).$$
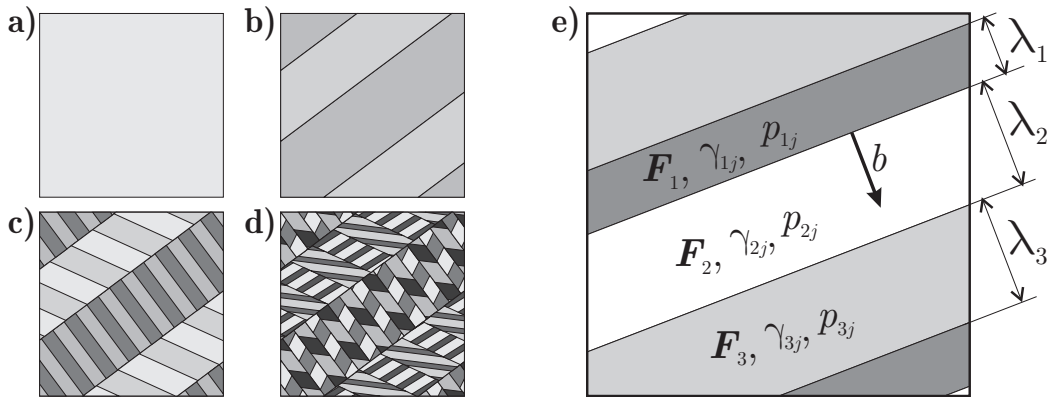

Figure 1: Schematic view of laminate refinement: a) homogeneous state, b) first- , c) second-, d) third-order laminate; e) first-order laminate for $N = 3$ with interface normal vector $\boldsymbol{b}$.

As experiments indicate that laminate microstructures often only comprise two distinct laminate domains (Dmitrieva et al., 2009), we will restrict our considerations in the sequel to a two-domain laminate only, i.e., $N = 2$, where λ will denote the volume fraction of phase 2.

4 Dissipation potentials and evolution equations

Dissipation occurs as a result of dislocation motion and is hence linked to changes of the plastic slip. A common definition of the dissipation functional, with the abbreviation $\boldsymbol{\gamma} = \{\gamma_{ij}\}$, is

$$\Delta(\dot{\boldsymbol{\gamma}}) = r\,||\dot{\boldsymbol{F}}_{\mathrm{p}}\boldsymbol{F}_{\mathrm{p}}^{-1}||, \tag{23}$$

with a positive constant r, the critical resolved shear stress, and the Euclidean norm defined by $||\boldsymbol{F}||^2 = \mathrm{tr}\,(\boldsymbol{F}^T\boldsymbol{F})$. For n active slip systems we infer

$$\Delta(\dot{\boldsymbol{\gamma}}) = r\,\sqrt{\sum_i^n \sum_j^n \dot{\gamma}_i\,\dot{\gamma}_j\,\boldsymbol{s}_i\cdot\boldsymbol{s}_j\,\boldsymbol{m}_i\cdot\boldsymbol{m}_j}, \tag{24}$$

so that for the special case of only two active slip systems within a common glide plane one concludes

$$\Delta(\dot{\gamma}_1, \dot{\gamma}_2) = r\,\sqrt{\dot{\gamma}_1^2 + \dot{\gamma}_2^2 + 2\dot{\gamma}_1\dot{\gamma}_2\,\boldsymbol{s}_1\cdot\boldsymbol{s}_2} \tag{25}$$

and for a single active slip system

$$\Delta(\dot{\gamma}) = r\,|\dot{\gamma}|. \tag{26}$$

Many approaches to model the microstructure evolution have been based on a condensed energy functional (12), which makes use of the dissipation distance (11). Besides, even the present, incremental approach requires the dissipation distance to capture the dissipation due to changes of the laminate volume fractions correctly. For a time step $[t_n, t_{n+1}]$ the dissipation distance is obtained from

$$D(\boldsymbol{\gamma}_{n+1}, \boldsymbol{\gamma}_n) = r\,\inf_{\boldsymbol{\gamma}(t)}\left\{\int_{t_n}^{t_{n+1}} \Delta(\dot{\boldsymbol{\gamma}})\,\mathrm{d}t \,:\, \boldsymbol{\gamma}(t_n) = \boldsymbol{\gamma}_n, \boldsymbol{\gamma}(t_{n+1}) = \boldsymbol{\gamma}_{n+1}\right\}. \tag{27}$$

For general problems with more than one active slip system, analytical integration of (27) to yield a closed-form expression for the dissipation distance does not appear feasible and approximations must be employed (Kochmann and Hackl, 2009a). Only for a single active slip system the dissipation distance can easily be obtained as

$$D(\gamma_{n+1}, \gamma_n) = r\,|\gamma_{n+1} - \gamma_n|. \tag{28}$$

One possible approximation for multiple slip systems has been introduced (Kochmann and Hackl, 2009a) analogously as

$$D(\boldsymbol{\gamma}_{n+1}, \boldsymbol{\gamma}_n) = r\,\sum_i^n |\gamma_{i,n+1} - \gamma_{i,n}|, \tag{29}$$

which is based on the assumption of non-interacting slip on the diverse active slip systems. Alternatively, one can make use of a the following approximation which is valid for arbitrary changes of the slips as long as the time step is kept sufficiently small

$$D(\boldsymbol{\gamma}_{n+1}, \boldsymbol{\gamma}_n) = r\,\sqrt{\sum_i^n \sum_j^n (\gamma_{i,n+1} - \gamma_{i,n})\,(\gamma_{j,n+1} - \gamma_{j,n})\,\boldsymbol{s}_i\cdot\boldsymbol{s}_j\,\boldsymbol{m}_i\cdot\boldsymbol{m}_j}. \tag{30}$$

For a material with microstructure, not only the energy density but also the dissipation potential must be given in its relaxed form, which has been proposed for the first-order laminate as follows (Hackl and Kochmann, 2008)

$$\Delta^*(\lambda, \boldsymbol{\gamma}, \dot{\lambda}, \dot{\boldsymbol{\gamma}}) = r\,\left[(1 - \lambda)\Delta(\dot{\gamma}_{1i}) + \lambda\,\Delta(\dot{\gamma}_{2i}) + |\dot{\lambda}|\,D(\gamma_{ij})\right]. \tag{31}$$

The first and second term represent dissipation due to changes of the plastic slips within the two laminate domains, and the third term characterizes the amount of dissipation due to changes of the volume fractions, i.e., the dissipated

energy necessary to transform e.g. a small part belonging to phase 1 into a part of phase 2 if λ increases. For a single active slip system the relaxed dissipation potential reduces to

$$\Delta^*(\lambda, \gamma_1, \gamma_2, \dot{\lambda}, \dot{\gamma}_1, \dot{\gamma}_2) = r\left((1-\lambda)|\dot{\gamma}_1| + \lambda|\dot{\gamma}_2| + \left|\dot{\lambda}(\gamma_1 - \gamma_2)\right|\right). \tag{32}$$

For multiple active slip systems the above discussion applies and approximations for the dissipation distance to account for dissipation due to volume fraction changes must be employed. For two active slip systems, we have proposed, following (29),

$$D(\boldsymbol{\gamma}) = r\left(|\gamma_{11} - \gamma_{21}| + |\gamma_{12} - \gamma_{22}|\right). \tag{33}$$

Another formulation results from (30) by making use of the assumption of an infinitesimally small time increment. Then, one obtains the alternative formulation

$$D(\boldsymbol{\gamma}) = r\sqrt{(\gamma_{11} - \gamma_{12})^2 + (\gamma_{21} - \gamma_{22})^2 + 2(\gamma_{11} - \gamma_{12})(\gamma_{21} - \gamma_{22})\,\boldsymbol{s}_1 \cdot \boldsymbol{s}_2}. \tag{34}$$

Note that this approximation (34) is obtained from assuming a negligibly small time increment, with no assumption made about the slip increments, i.e. this approximation can be used also for the onset of lamination when the jump of the plastic slip in the second laminate domain can be quite considerable but the time increment is small.

Now that we have established representations both for the relaxed energy (21) and for the relaxed dissipation potential (31) with (34), we attack the problem of modeling the evolution of laminates by making use of an incremental strategy. Via the principle given in (7) we obtain evolution equations for λ and γ_{ij} in terms of the stationarity conditions to minimize the above Lagrange functional, being

$$0 \in \frac{\partial \Psi^{\text{rel}}}{\partial \lambda} + \frac{\partial \Delta^*}{\partial \dot{\lambda}}, \tag{35}$$

$$0 \in \frac{\partial \Psi^{\text{rel}}}{\partial \gamma_{ij}} + \frac{\partial \Psi^{\text{rel}}}{\partial p_{ij}} \operatorname{sign} \dot{\gamma}_{ij} + \frac{\partial \Delta^*}{\partial \dot{\gamma}_{ij}}, \quad \text{for all } 1 \le i \le N,\ 1 \le j \le n. \tag{36}$$

To compute the evolution of plastic microstructures in time, we have proposed an incremental formulation for the numerical treatment of (35) and (36) (Hackl and Kochmann, 2008), using specified finite deformation increments $[\boldsymbol{F}_n, \boldsymbol{F}_{n+1}]$ with known initial conditions $\boldsymbol{F}_n$, $\gamma_{ij,n}$, λ_n, $p_{ij,n}$ and the known deformation $\boldsymbol{F}_{n+1}$ at the end of the time step. Then, (35) and (36) can be used to compute the updates $\Delta\gamma_{ij} = \gamma_{ij,n+1} - \gamma_{ij,n}$, $\Delta\lambda = \lambda_{n+1} - \lambda_n$ and $\Delta p_{ij} = p_{ij,n+1} - p_{ij,n}$ for given $\Delta\boldsymbol{F} = \boldsymbol{F}_{n+1} - \boldsymbol{F}_n$ in a staggered algorithm. Also, the model accounts for laminate rotation (Hackl and Kochmann, 2009) and updates the hardening variables due to volume fraction changes (Hackl and Kochmann, 2008). For details of the numerical implementation and the exact algorithmic realization see (Hackl and Kochmann, 2008; Kochmann and Hackl, 2009a).

5 Results

It has been reported (Hackl and Kochmann, 2009) that the present model gives rise to interesting effects when applied to cyclic loading of single-crystals in terms of an elastic shakedown, i.e. the stress-strain behavior has been shown to rapidly reduce within a few number of cycles (less than four) to almost elastic behavior with an almost steady laminate. However, it has been argued that this short number of cycles until the steady state is reached is rather unphysical. Therefore, we investigate here the influence of work hardening on the cyclic loading of single-crystals by computing the stress-strain behavior at the material point level.

5.1 Cyclic loading in single-slip plasticity

Let us first analyze the cyclic load response of a crystal in two dimensions with only a single active slip system, whose orientation is defined by the angle φ through $\boldsymbol{s} = (\cos\varphi, \sin\varphi, 0)^T$, $\boldsymbol{m} = (-\sin\varphi, \cos\varphi, 0)^T$. The material is subject to the homogeneous deformation

$$\boldsymbol{F}(\gamma) = \begin{pmatrix} 1 & \gamma & 0 \\ 0 & 1 & 0 \\ 0 & 0 & 1 \end{pmatrix}, \tag{37}$$

so that we can study the evolution of the microstructure, of the energy and, of course, of the shear stress as functions of the shear strain γ. It becomes apparent from Figure 2 that hardening does indeed considerably affect the cyclic
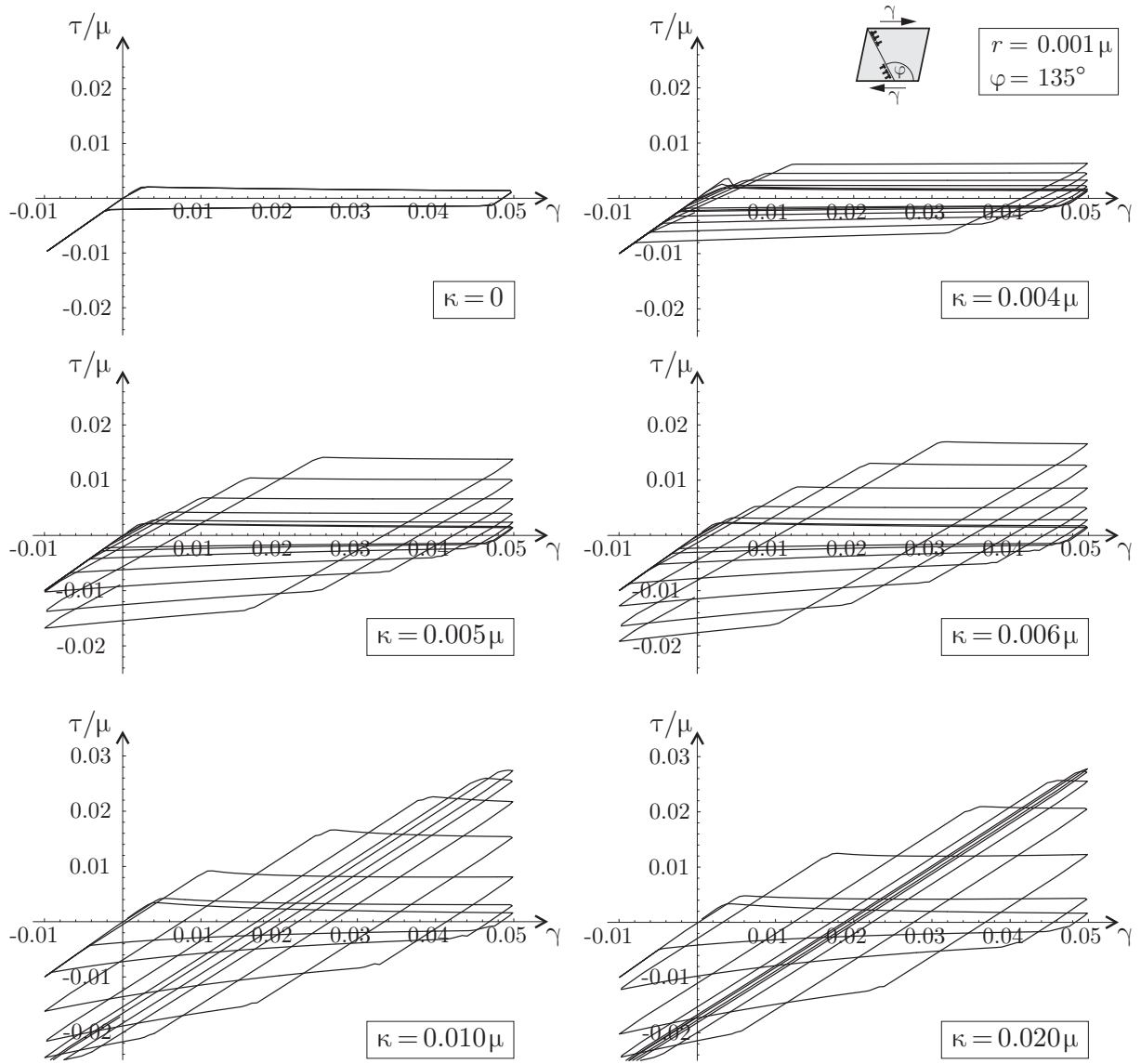
Figure 2: Stress-strain curves for a cyclic shear test for various hardening moduli κ and fixed remaining properties (shown are the first seven complete cycles).

load behavior: Without hardening ($\kappa = 0$) the stress-strain hysteresis remains unaltered for all cycles. Note that the nonconvexity of the free energy density for the chosen slip system orientation of $\varphi = 135°$ appears only for $\gamma > 0$ such that we observe microstructure formation and the typical corresponding stress plateau only in that region, whereas for $\gamma < 0$ the body deforms homogeneously and no microstructure forms. With an increasing amount of hardening ($\kappa > 0$) the stress-strain behavior changes essentially. For higher load cycles, the hysteresis becomes narrower and the stresses increase. The final elastic shakedown becomes visible for high hardening parameters (see e.g. the curves for $\kappa = 0.01\mu$ and $\kappa = 0.02\mu$). Here, one can clearly state that the amount of hardening essentially affects the progressive degeneration of the stress-strain hysteresis by altering the number of load cycles required until the final steady state is reached. For moderate hardening it may hence take a large number of load cycles until the elastic shakedown occurs.

The observed stress-strain behavior can be linked to microstructural mechanisms by inspection of the evolving internal variables. Figure 3 illustrates the evolution of the plastic slips, the volume fractions and the stored energy as functions of the applied shear strain for little hardening only ($\kappa = 0.004\mu$), whereas Figure 4 illustrates the course of the same quantities for strong hardening ($\kappa = 0.02\mu$). In Figure 3 the paths of the internal variables of the first cycle considerably differ from those of subsequent cycles, but the changes between subsequent cycles after the first cycle are relatively small. Note that the plastic slips in both phases, γ_1 and γ_2, show distinct cyclic changes for the entire load path investigated here. Also, the volume fraction λ changes cyclically between 0 and approximately 10%. Hence, a laminate microstructure forms with both domains deforming plastically, which

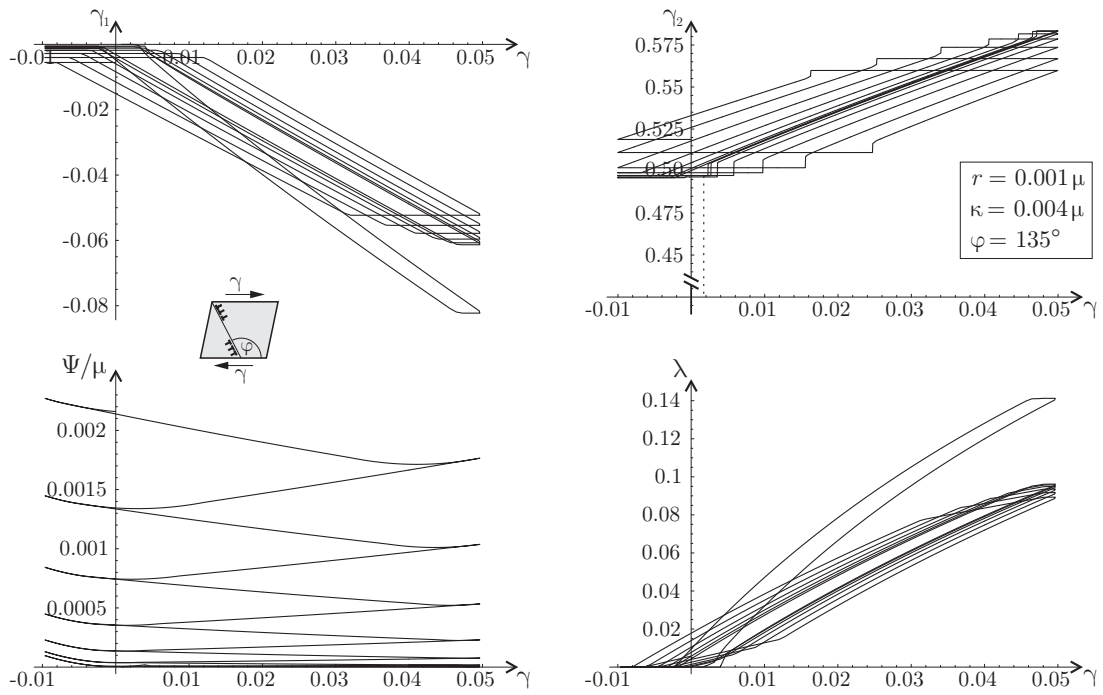Figure 3: Evolution of the internal variables (i.e., the plastic slips γ_1 and γ_2, and the volume fraction λ of phase 2) and of the energy during a cyclic shear test for little hardening ($\kappa = 0.004\mu$); shown are the first seven complete cycles.

forms and vanishes cyclically. As a result, the stored energy increases moderately from cycle to cycle due to the increasing amount of intrinsically stored energy captured in the monotonously increasing plastic hardening variables p_i.
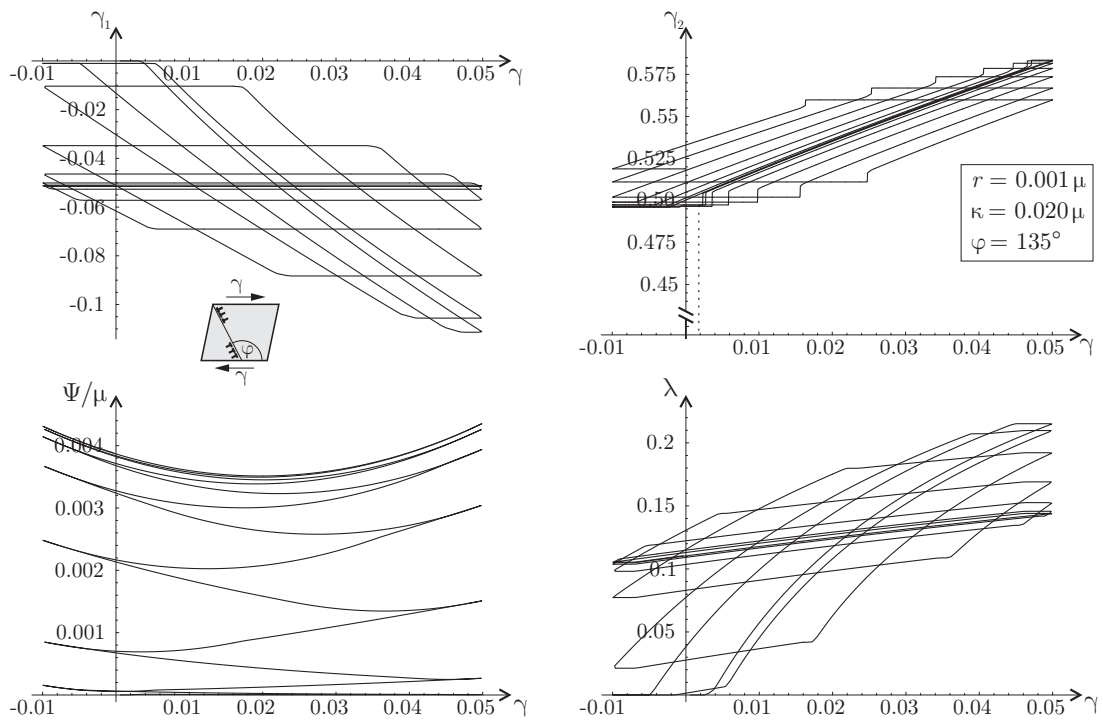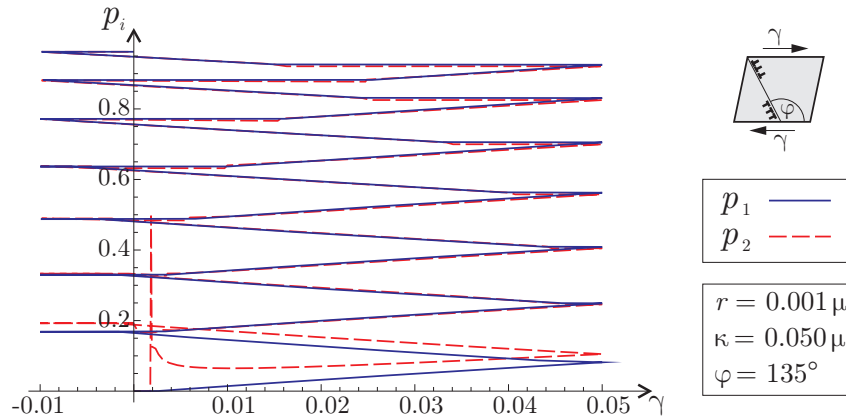

Figure 4: Evolution of the internal variables (i.e., the plastic slips γ_1 and γ_2, and the volume fraction λ of phase 2) and of the energy during a cyclic shear test for high hardening ($\kappa = 0.02\mu$); shown are the first seven complete cycles.

Figure 5: Evolution of the hardening variables p_1 and p_2 during cyclic loading in single-slip.

In contrast, Figure 4 indicates a different behavior for large hardening (here, $\kappa = 0.02\mu$). Again, we observe that the evolution of the internal variables changes with an increasing number of load cycles, and the plot of the evolving plastic slip γ_2 in the second laminate domain is almost identical to the one of Figure 3. However, two crucial differences become obvious: now, the plastic slip γ_1 in the initial laminate domain transforms within a few load cycles to reach a steady value of about 5%, which hardly changes during subsequent load cycles, i.e. the initial laminate domain transforms into a steady, elastic state after a few cycles only. Besides, the evolution of the volume fraction λ also indicates a drastic change. In constrast to the periodic changes in Figure 3, the volume fraction λ here very soon reaches an approximately steady state with only minor changes during subsequent cycles (viz., λ tends to change cyclically between about 10 and 12% only). The laminate thus considerably deviates from the one observed for small hardening only. Here, within a few cycles an approximately steady laminate is developed with hardly changing volume fractions, and only the smaller, newly-formed domain 2 exhibiting plastic flow. As a result, the stored energy increases notably faster than before and the elastic shakedown is reached after fewer load cycles.

Finally, let us complete the description of results by underlining the influence of the specific hardening formulation chosen here. To this end, we inspect the evolution of the hardening variables, as illustrated in Figure 5, where the evolution of p_1 and p_2 is plotted exemplarily for a laminate loaded cyclically in single-slip with the given set of material parameters. The graphic highlights two particular characteristics during the evolution of the hardening variables, which shall be discussed briefly.

On the one hand, the impact of the update procedure for the hardening variables becomes apparent from the evolution of p_2 upon laminate nucleation, as has been reported e.g. in (Hackl and Kochmann, 2009; Kochmann and Hackl, 2009b). During the initial positive loading of the first load cycle, we have $p_1 \cong |\gamma_1|$ due to the present flow rule and the monotonically increasing load. As the second laminate phase forms during the first load cycle, we observe that p_2 first assumes the value $|\gamma_2|$ upon laminate initiation, but then rapidly decreases from its initial value and gradually approaches the evolving p_1-value due to the evolution of the volume fractions and the corresponding updates of the hardening variables. At the end of the first cycle, both hardening variables show approximately equal values, from where on we observe uniform hardening in both laminate phases.

On the other hand, we can observe in Figure 5 how both hardening variables increase with subsequent load cycles, i.e. with repeated plastic deformation, which gives rise to the observed cyclic hardening and eventually to the elastic shakedown of the stress-strain hysteresis. This is a major advantage of the present variational formulation, which allows for the study of cyclic loading, while the literature approach, based on condensed energy functionals, accounts for monotonic loading. Here, the values of the hardening variables gradually increase during each load cycle, leading to higher stresses and the reported cyclic hardening. Note that the orientation (characterized by vector $\boldsymbol{b}$) shows hardly any changes during load cycles due to the large amount of dissipation required to rearrange the rotated laminate. Therefore, the nucleated laminate microstructures predominantly remains in its initial orientation, which results from the energetically optimal state upon laminate formation.

5.2 Cyclic loading in double-slip plasticity

When more than one slip system is active, latent hardening due to interaction mechanisms (such as cross slip) plays an essential role, increasing the amount of work hardening considerably. To illustrate this effect, we show results for a cyclic shear test with two active slip systems within the same slip plane, so that (14) holds. For comparison with the single-slip results, we locate the slip plane under an angle of $\varphi = 135°$ and align the two active slip systems under angles ψ_1 and ψ_2 with respect to the direction of shear, as depicted in the schematic view included in Figure 6. The particular hardening characteristics are described in terms of the hardening parameters κ_{ij} in (15).
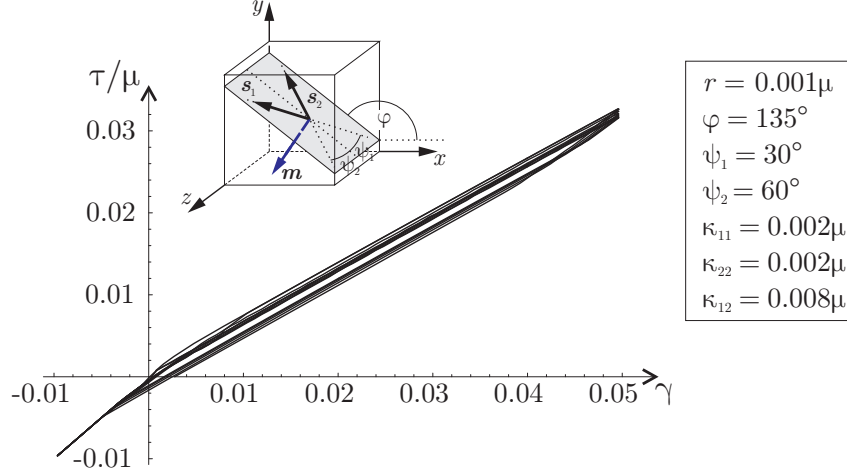

Figure 6: Cyclic stress-strain response for double-slip plasticity with low hardening (shown are the first seven load cycles) for non-symmetric active slip systems.

Figure 6 illustrates the stress-strain behavior for two active slip systems with low (self- and latent) hardening. We observe the typical stress-strain hysteresis with only little cyclic deviations, as has already been noted for the single-slip problem with a low hardening parameter κ (see Figure 2). Here, the asymmetrically aligned slip systems ($\psi_1 \neq \psi_2$) locates the resultant slip out-of-plane (and so is the laminate orientation), which gives rise to the enormous increase of the stress even for low values of the hardening parameters κ_{ij}.
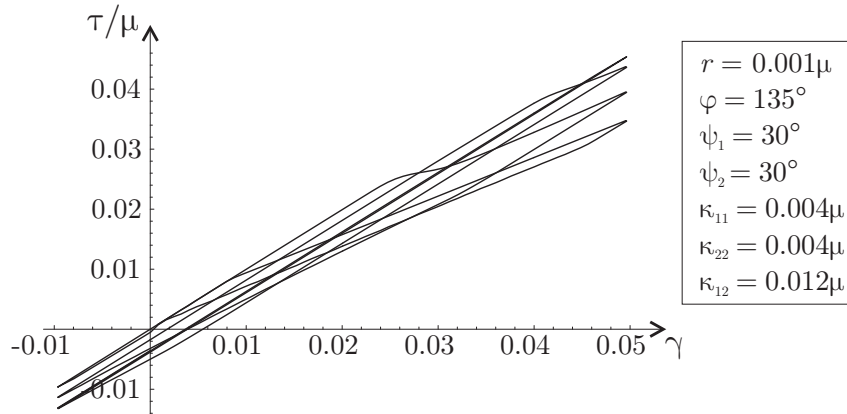

Figure 7: Cyclic stress-strain response for double-slip plasticity with high hardening (shown are the first seven load cycles) for symmetric active slip systems.

In contrast, Figure 7 shows the analogous stress-strain curve with higher hardening parameters κ_{ij}. Here, the stress-strain curve shows a similar hysteresis loop, which, however, is not completely recovered but, upon further load cycles, deviates gradually. Within a few load cycles the typical, aforementioned elastic shakedown appears due to the increase of energy as a consequence of work hardening and, in particular, latent hardening of the two active slip systems. In conclusion, the presence of hardening, as for the examples in single-slip plasticity, considerably effects the cyclic stress-strain behavior and determines the number of cycles required before the laminate microstructure degenerates to approach a close to elastic mechanical behavior.

6 Conclusions

We have outlined an incremental, variational approach to model the evolution of laminate microstructures in single- and multi-slip plasticity of single crystals, and we have applied this formulation to investigate the cyclic loading in single- and double-slip. The influence of work hardening on the cyclic stress-strain response has been proved crucial to affect the degeneration of the elastoplastic hysteresis loop with an increasing number of load cycles. For single-slip plasticity, the hardening parameter (introduced as a scaling factor of the intrinsically stored energy) shows a critical impact on the number of load cycles required until a final, steady laminate has formed. This has been explained by the different evolving laminate characteristics for strong work hardening vs. little hardening only.

For double-slip plasticity, the presence of work and latent hardening has been shown to yield the (qualitatively) same impact on the stress-strain response, as hardening accelerates the degeneration of the hysteresis loop to very quickly yield the elastic shakedown, which had been reported before.

In conclusion, work hardening (self-hardening as well as latent hardening in the presence of more than one active slip system) considerably affects the cyclic load behavior, by changing the microstructural characteristics and, as a consequence, the stress-strain hysteresis. With increasing influence of hardening, the laminate microstructure more readily transforms into an almost steady final state, which deforms close to elastically.

References

Biot, M. A.: *Mechanics of Incremental Deformations*. John Wiley & Sons Inc., New York (1965).

Carstensen, C.; Hackl, K.; Mielke, A.: Non-convex potentials and microstructures in finite-strain plasticity. *Proc. Royal Soc. London*, A458, (2002), 299 – 317.

Carstensen, C.; Conti, S.; Orlando, A.: Mixed analytical-numerical relaxation in finite single-slip crystal plasticity. *Continuum Mech. Thermodyn.*, 20, (2008), 275 – 301.

Christian, J. W.; Mahajan, S.: Deformation twinning. *Progr. Mater. Sci.*, 39, (1995), 1 – 157.

Ball, J. M.: Convexity Conditions and Existence Theorems in Nonlinear Elasticity. *Arch. Rat. Mech. Anal.*, 63, (1977), 337 - 403.

Ball, J. M.; James, R. D.: Fine phase mixtures as minimizers of energy. *Arch. Rat. Mech. Anal.*, 100, (1987), 13 – 52.

Bartels, S.; Carstensen, C.; Hackl, K.; Hoppe, U.: Effective Relaxation for Microstructure Simulations: Algorithms and Applications. *Comp. Meth. Appl. Mech. Eng.*, 193, (2004), 5143 - 5175.

Conti, S.; Ortiz, M.: Minimum principles for the trajectories of systems governed by rate problems. *J. Mech. Phys. Solids*, 56, (2008), 1885 – 1904.

Conti, S.; Theil, F.: Single-slip elastoplastic microstructures. *Arch. Rat. Mech. Anal.*, 178, (2005), 125 – 148.

Dmitrieva, O.; Dondl, P. W.; Müller, S.; Raabe, D.: Lamination microstructure in shear deformed copper single crystals. *Acta Mater.*, 57, (2009), 3439 – 3449.

Dolzmann, G.: Numerical Computation of Rank-One Convex Envelopes. *SIAM J. Num. Anal.*, 36, (1999), 1621 - 1635.

Dolzmann, G.: *Variational Methods for Crystalline Microstructure Analysis and Computation*. Springer-Verlag, Berlin, 2003.

Ericksen, J. L.: Equilibrium of bars. *J. Elasticity*, 5, (1975), 191 – 201.

Germain, P.: *Cours de Mécanique des Milieux Continus*. Masson et Cie, Paris, 1973.

Govindjee, S.; Mielke, A.; Hall, G. J.: The free energy of mixing for n-variant martensitic phase transformations using quasi-convex analysis. *J. Mech. Phys. Solids*, 51, (2003), 1 – 26.

Hackl, K.; Fischer, F. D.: On the relation between the principle of maximum dissipation and inelastic evolution given by dissipation potentials. *Proc. Royal Soc. London*, A464, (2007), 117 - 132.

Hackl, K.; Mielke, A.; Mittenhuber, D.: Dissipation distances in multiplicative elastoplasticity. In: Wendlang, W. L., Efendiev, M. (eds.), Analysis and Simulation of Multifield Problems. Springer (2003), New York.

Hackl, K., Kochmann, D. M.: Relaxed potentials and evolution equations for inelastic microstructures. In: *Theoretical, Computational and Modelling Aspects of Inelastic Media*, B. Daya Reddy, ed., Springer, Berlin, 2008.

Hackl, K.; Kochmann, D. M.: An incremental strategy for modeling laminate microstructures in finite plasticity – energy reduction, laminate orientation and cyclic behavior. In: *Lecture Notes in Applied and Computational Mechanics*, E. Ramm, ed., in press, 2009.

Jin, N. Y.; Winter, A. T.: Dislocation structures in cyclically deformed [001] copper crystals. *Acta Met.*, 32, (1984), 1173 – 1176.

Kochmann, D. M.; Hackl, K.: Time-continuous evolution of microstructures in finite plasticity. In: *Variational Concepts with Applications to the Mechanics of Materials*, K. Hackl, ed., Springer, Berlin, in press, 2009a.

Kochmann, D. M.; Hackl, K.: The evolution of laminates in finite crystal plasticity – a variational approach. *Contin. Mech. Thermodyn.*, submitted for publication, 2009b.

Kohn, R.: The relaxation of a double-well problem. *Continuum Mech. Thermodyn.*, 3, (1991), 193 – 236.

Lambrecht, M.; Miehe, C.; Dettmar, J.: Energy relaxation of non-convex incremental stress potentials in a strain-softening elastic-plastic bar. *Int. J. Solids Struct.*, 40, (2003), 1369 – 1391.

Miehe, C.; Schotte, J.; Lambrecht, M.: Homogenization of inelastic solid materials at finite strains based on incremental minimization principles. Application to the texture analysis of polycrystals. *J. Mech. Phys. Solids*, 50, (2002), 2123 – 2167.

Miehe, C.; Lambrecht, M.; Gürses, E.: Analysis of Material Instabilities in Inelastic Solids by Incremental Energy Minimization and Relaxation Methods: Evolving Deformation Microstructures in Finite Plasticity. *J. Mech. Phys. Solids*, 52, (2004), 2725 – 2769.

Mielke, A.: Finite elastoplasticity, Lie groups and geodesics on SL(d). In: *Geometry, Dynamics, and Mechanics*, P. Newton ; A. Weinstein; P. Holmes, eds., Springer, Berlin, 2002.

Mielke, A.: Deriving new evolution equations for microstructures via relaxation of variational incremental problems. *Comp. Meth. Appl. Mech. Eng.*, 193, (2004), 5095 – 5127.

Mielke, A.; Ortiz, M.: A class of minimum principles for characterizing the trajectories and the relaxation of dissipative systems. *ESAIM: Control, Optimization and Calculus of Variations*, 14, (2007), 494 – 516.

Morrey, C. B.: Quasi-Convexity and the Lower Semicontinuity of Multiple Integrals. *Pacific J. Math.*, 2, (1952), 25 - 53.

Nguyen, Q. S.: *Stability and Nonlinear Solid Mechanics*. John Wiley & Sons, New York, 2000.

Ortiz, M.; Repetto, E. A.: Nonconvex energy minimization and dislocation structures in ductile single crystals. *J. Mech. Phys. Solids*, 47, (1999), 397 – 462.

Ortiz, M.; Repetto, E. A.; Stainier, L.: A theory of subgrain dislocation structures. *J. Mech. Phys. of Solids*, 48, (2000), 2077 – 2114.

Truskinovsky, L.; Zanzotto, G.: Finite-scale microstructures and metastability in one-dimensional elasticity. *Meccanica*, 30, (1995), 577 – 589.

Ziegler, H.; Wehrli, C.: The Derivation of Constitutive Relations from the Free Energy and the Dissipation Function. In: *Advances in Applied Mechanics*, vol. IV, Th. Y. Wu; J. W. Hutchinson, eds., Academic Press Inc., 1987.

Address: Dr.-Ing. Dennis M. Kochmann and Prof. Dr. rer. nat. Klaus Hackl, Ruhr-Universität Bochum, Lehrstuhl für Allgemeine Mechanik, D-44780 Bochum
email: `dennis.kochmann@rub.de`; `klaus.hackl@rub.de` .